Journal of Materials Processing Tech. 311 (2023) 117817

Contents lists available at ScienceDirect

Journal of Materials Processing Tech.

journal homepage: www.elsevier.com/locate/jmatprotec

Humidity control in laser powder bed fusion using titanium alloy powder for quality assurance of built parts and reusability of metal powder

Mitsugu Yamaguchi [a,*], Kotaro Kushima [b], Yushi Ono [c], Tomohiro Sugai [c], Tomohiro Oyama [c], Tatsuaki Furumoto [a]

[a] Advanced Manufacturing Technology Institute (AMTI), Kanazawa University, Kakuma-machi, Kanazawa, Ishikawa 920-1192, Japan
[b] Graduate School of Natural Science and Technology, Kanazawa University, Kakuma-machi, Kanazawa, Ishikawa 920-1192, Japan
[c] Innovation Unit, Taiyo Nippon Sanso Corporation, 3054–3, Shimokurosawa, Takane-cho, Hokuto-shi, Yamanashi 408-0015, Japan

ARTICLE INFO

Associate Editor: Jingjing Li

Keywords:
Additive manufacturing
Laser-based powder bed fusion
Titanium alloy
Oxygen concentration
Humidity
Reusability

ABSTRACT

This study investigated the influence of oxygen concentration and humidity in a laser power bed fusion system on the building aspects of titanium alloy powder for the quality assurance of built parts and the reusability of metal powders. Controlling the humidity inside the building chamber was found to be more important than controlling the oxygen concentration to prevent the oxidation of the built part and metal powder. Low oxygen concentration and humidity resulted in high circularity and a narrow size distribution of spatter particles. The oxidation of spatter particles was accelerated with an increase in the oxygen and humidity levels within the building chamber, particularly with an increase in humidity. High oxygen concentration and humidity caused a change in the Marangoni convection, resulting in the formation of defects inside the built part. Oxygen was captured by spatter particles or built parts during the liquid phase, and the degrees of influence of the oxygen concentration and humidity in the building chamber on the capture of oxygen were similar. The oxygen content of the built part had a greater effect on the mechanical properties of the built part, as compared with the hydrogen content. The Charpy impact strength was sensitive to the capture of oxygen and humidity by the built part and could effectively help understand the building aspects under slightly different building environments. This study demonstrates that maintaining the oxygen and humidity conditions below 10 ppm is indispensable for building chambers.

1. Introduction

A metal-based laser powder bed fusion (PBF-LB/M) system enables the manufacturing of complex functional geometries in various industries, especially in aerospace and medicine, where this technique is used to enhance weight-saving production and reduce the number of parts (Schmidt et al., 2017). Another advantage of the PBF-LB/M system is the recyclability of the unused powder deposited around the built parts. However, this technique requires a high-power heat source to complete the building process, generating metal vapour jets and spatter particles. The contamination of such oxidised particles in the powder bed can affect the reusability of the powder. Harkin et al. (2020) investigated the influence of the reuse times on the oxidation extent of the powder using an inert gas fusion method and showed that the maximum oxygen limit of 0.13 wt% was exceeded after eight reuses, resulting in a degradation of the extra-low interstitial Ti–6Al–4V powder from Grade 23. In addition, from the morphology observation of the powder, Seyda et al. (2012) revealed that the average particle size of a Ti–6Al–4V virgin powder was 37.4 μm and increased to 51.2 μm after 12 reuse times, which was attributed to the sintering between the powders due to residual heat. Furthermore, Williams et al. (2021) investigated the effect of the oxidation extent of the powder on the mechanical properties of the built part and showed that the oxidised particles incorporated into a Ti–6Al–4V part negatively impact the mechanical properties of the part owing to mechanical defects (oxide films/residue) and local chemical changes (interstitial impurities) by an element/chemical state analysis. These results suggest that to enhance the reusability of the powder and the mechanical properties of the built part, process conditions and the building environment should be appropriately selected.

Titanium alloys such as Ti–6Al–4V have excellent mechanical properties, corrosion resistance, and biocompatibility and are widely

* Corresponding author.
E-mail address: yamaguchi@se.kanazawa-u.ac.jp (M. Yamaguchi).

https://doi.org/10.1016/j.jmatprotec.2022.117817
Received 12 July 2022; Received in revised form 26 October 2022; Accepted 6 November 2022
Available online 7 November 2022
0924-0136/

used in additive manufacturing (Shipley et al., 2018). However, the microstructure and properties of titanium alloys are sensitive to the capture of interstitial impurities such as oxygen. Yan et al. (2014) investigated the factors that decrease the ductility of the as-sintered Ti–6Al–4V containing more than approximately 0.33% oxygen by using a transmission electron microscope (TEM) and three-dimensional atom probe tomography and found three microstructural changes: formation of acicular α precipitates in the β phase, precipitation of the α_2-type of nano-scaled clusters (Ti_3Al) in the α matrix, and an interface-stabilized layered structure of α-β-α between the α grains. The capture of oxygen is also a well-known issue for Ti–6Al–4V powder in the PBF-LB/M process. The factors related to the environment in which the powder and built part are oxidised are the oxygen and humidity conditions in the building atmosphere, although some amount of oxygen penetrates the powder during its granulation process. Hryha et al. (2016) investigated the oxidation extent of Ti–6Al–4V powder obtained via a gas atomised process using an X-ray photoelectron spectroscopy (XPS), and the oxide film thickness reached 4.2 nm even under highly pressurised argon gas. Several studies have examined the influence of the building environment in the PBF-LB/M system on the capture of oxygen in the powder and built parts. In particular, this process is implemented under high temperatures exceeding the melting point, and reactivity with oxygen can increase with the building environment. Pauzon et al. (2021) investigated the influence of the oxygen concentration in the building atmosphere on the oxygen content in the Ti–6Al–4V part using XPS and revealed that the oxygen content in the built part increased with the oxygen concentration in the building atmosphere. In addition, Quintana et al. (2018) compared the oxygen content in Ti–6Al–4V powders with the reuse times using an inert gas fusion method and showed that the oxygen content in the virgin powder was 0.09 wt% and reached 0.13 wt% with an increase in the reuse times due to the mixture of oxidised spatter particles even when the oxygen concentration was below 100 ppm. These results indicate that the oxygen concentration in the building atmosphere and reuse times affect the oxygen content in the reuse powder and built parts.

Meanwhile, Cordova et al. (2020) prepared Ti–6Al–4V powder with four humidity levels—virgin, drying in vacuum and air, and moisturising treatments—and investigated the influence of the moisture content on the powder characteristics. They showed that the powders agglomerated owing to a liquid bridge after the moisturising treatment at 323 K and 80% relative humidity, resulting in a reduction in the flowability. Several studies have examined that the influence of the moisture in the powder on hydrogen porosity during the building process. To limit the appearance of porosity resulting from the presence of hydrogen, it is important to reduce the humidity in the building environment. Weingarten et al. (2015) proposed a double scan method for the pre-drying treatment. The first scan was carried out with a low-power laser, resulting in the sintering of the powder, after which the second scan melted the powder, leading to a reduction in porosity. In addition, Li et al. (2016) investigated the influence of the drying process on the porosity using XPS and X-ray microscopy and found that the drying of the powder prevented the formation of deleterious oxide and hydroxide during the building due to the modification of powder surface by removing moisture during the drying process. These results suggest that humidity in the building atmosphere affects the reuse powder characteristics and the formation of pores inside the built parts.

To ensure the quality of built parts and enhance the reusability of the unmelted powder in the PBF-LB/M process of Ti–6Al–4V powder, strict control of the oxygen and humidity conditions of the powder feedstock, powder storage, building environment, and post-processing is required. Previous studies have shown that the presence of undesirable impurities, such as oxygen and hydrogen, negatively affects the powder characteristics and mechanical properties of the built part. However, the influence of the humidity in the building environment on the oxygen and hydrogen content, porosity, and mechanical properties of built parts has not been adequately explained. This study addresses these deficiencies, in addition to providing novel findings regarding the influence of humidity on the morphology, particle size distribution, and reusability of the spatter particles. Specifically, this study investigated the principal factors affecting the oxidation of built parts and reusability of the powder when the Ti–6Al–4V powder was prepared using a PBF-LB/M system under different building environment parameters, such as oxygen concentration and humidity inside the building chamber. Finally, a building strategy is proposed for the quality assurance of built parts and better reuse of unmelted powders.

2. Material and method

The morphology of the metal powder, as determined using SEM, and its particle size distribution are shown in Fig. 1. The powder was a spherical titanium alloy (Ti–6Al–4V Grade 23), manufactured via a plasma atomisation process; it featured a spherical morphology with particle diameters (D_{10}–D_{90}) in the range of 27–57 μm and a median diameter (D_{50}) of 38 μm. The moisture content in the metal powders was measured using a Karl Fischer moisture metre (Nittoseiko Analytech Co., Ltd.; CA31), and the amount of moisture before building was controlled at 20 ppm using a dryer (Taiyo Nippon Sanso Corp.: 3DPro Powder Drying Cabinet). Table 1 presents the experimental conditions. The oxygen concentration and humidity inside the building chamber were controlled using a build gas circulating purifier (Taiyo Nippon Sanso Corp.: 3DPro PrintPure™) connected to a commercial PBF-LB/M system (GE Additive: Concept Laser M2). The gas circulating purifier comprised a fully sealed blower and two adsorption columns to remove oxygen and moisture. A portion of the atmospheric gas inside the building chamber was drawn through a bypass line and introduced into the adsorption columns and then the purified gas returned to the building chamber. The oxygen concentration and humidity were monitored using an oxygen/humidity metre (Michell Instruments Ltd.: XGA301 Industrial Gas Analyser). Some of the atmospheric gas inside the building chamber was drawn at a flow rate of 2 L/min using a pump and introduced into the metre. The oxygen concentration and humidity inside the building chamber were controlled to remain under 10 ppm using the build gas circulating purifier and oxygen/humidity metre. The substrate was pure titanium (Grade 2), and the building surface was sandblasted to achieve a surface roughness of $Ra = 2.0$ μm. The process parameters were adjusted to achieve the highest density of the built part, with a laser power of 370 W, laser scan speed of 1500 mm/s, beam diameter of 0.18 mm, and hatch distance of 95 μm; thus, a layer thickness of 0.05 mm was realised. Following the building processes, the spatter particles were collected from the loose powder surface to observe their morphology and extent of oxidation. The circularity of the spatter particles was evaluated through image analyses using ImageJ, an open-source software. The SEM images of the spatter particles observed at a magnification of × 40 were binarized with a threshold value of 100. Subsequently, the particle area was measured as 6300–31500 μm^2 (particle size of 90–200 μm for a perfect circle), as shown in Fig. 2. The circularity of the spatter particles can be defined as

$$Circularity = \frac{4\pi \times Particle\ \ area}{Perimeter^2}, \tag{1}$$

where *Particle area* is the projected area detected using binarization, and *Perimeter* is the length of the outline of the spatter particles. The size of the spatter particles was defined as the length of the major axis, according to an elliptical approximation of the projected area. In addition, the spatter particles were sectioned and observed using a focused gallium ion beam-SEM (FIB-SEM) (Thermo Fisher Scientific, Inc.: Scios 2) and TEM (Thermo Fisher Scientific, Inc.: Tecnai). Five images were evaluated for each specimen, and the average values were considered. Furthermore, the oxygen and hydrogen contents in the built parts and the particles were analysed using an N/O/H analyser (Leco co., Ltd.: ON836, RHEN602). The built parts with dimensions of 9 mm × 9 mm

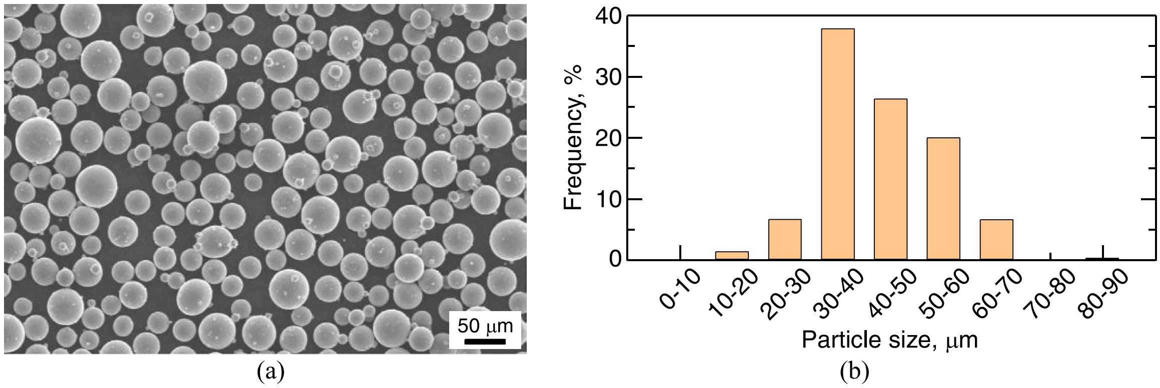

Fig. 1. Titanium alloy powder used: (a) SEM image and (b) particle size distribution.

Table 1
Experimental conditions.

Laser source		
Wavelength	nm	1070
Power	W	370
Beam diameter	mm	0.18
Laser scan speed	mm/s	1500
Substrate		Pure Ti (ASTM: Grade 2)
Surface roughness, *Ra*	μm	2.0
Metal powder		Ti–6Al–4V Grade 23
Shape		Spherical
Median diameter (D_{50})	μm	38
Layer thickness	μm	50
Building environment		
Oxygen concentration	ppm	10–1500
Humidity	ppm	10–1500

× 65 mm (1300 layers) were sectioned with dimensions of 3 mm^3, and 0.1 g of particles were prepared as the specimens. The specimens were placed in a graphite crucible and heated above the melting point using an impulse furnace. Subsequently, the oxygen in the specimens reacted with the graphite crucible to form CO and CO_2, which was detected using a non-dispersive infrared (NDIR) sensor. The gases flew through a heated reagent, and the CO was oxidised to form CO_2 and H was oxidised to form H_2O. Thereafter, the gases were detected using another set of NDIR sensors to determine both the oxygen and hydrogen contents. The porosity of the built parts with dimensions of 15 mm^3 (300 layers) was determined by analysing the image of the polished built surface captured using a metallurgical microscope (Olympus Co., Ltd.: GX71). Tensile and Charpy impact strength tests according to ASTM E8 and ASTM A 370 were conducted at 300 K using a universal testing machine (Shimadzu Corp.: AG-50KNI) and a Charpy impact testing machine (Yonekura Mfg. Co., Ltd.: 500-CI), respectively. The built parts with dimensions of φ15 mm × 90 mm (1800 layers) and 9 mm × 9 mm × 65 mm (1300 layers) were prepared as the specimens for the tensile and Charpy impact strength tests. Finally, the oxygen content of the metal powder after reaching a building volume of 250,000 mm^3 was investigated to evaluate the reusability of the metal powder. The reused powder was sieved to remove large spatter particles with sizes exceeding 100 μm and mixed with the virgin metal powder, in a reused powder-to-virgin powder ratio of 1:5.

3. Result and discussions

3.1. *Influence of oxygen concentration and humidity in the building environment on spatter particle morphology*

Fig. 3 depicts a comparison of the circularity of the spatter particles under different oxygen concentrations and humidity levels in the building chamber. At an oxygen concentration and humidity of 10 ppm, the spatter particles comprised a large proportion of the spherical powder with a circularity of 0.8 or higher. At 1500 ppm, a large proportion of the irregular powder exhibited a circularity of 0.7 or lower.

Fig. 4 shows a comparison of the size distribution of the spatter particles under different building environments. The median diameters (D_{50}) of the spatter particles were 137 μm and 134 μm at the oxygen concentration and humidity of 10 ppm and 1500 ppm, respectively. The mean diameter of the spatter particles was more than 3.5 times larger than that of the virgin powder (38 μm). The size distribution of spatter particles was significantly affected by the oxygen concentration and humidity, and these factors were observed to have a marked influence on the morphology of the spatter particles. When the oxygen concentration and humidity were 10 ppm and 1500 ppm, the proportion of the

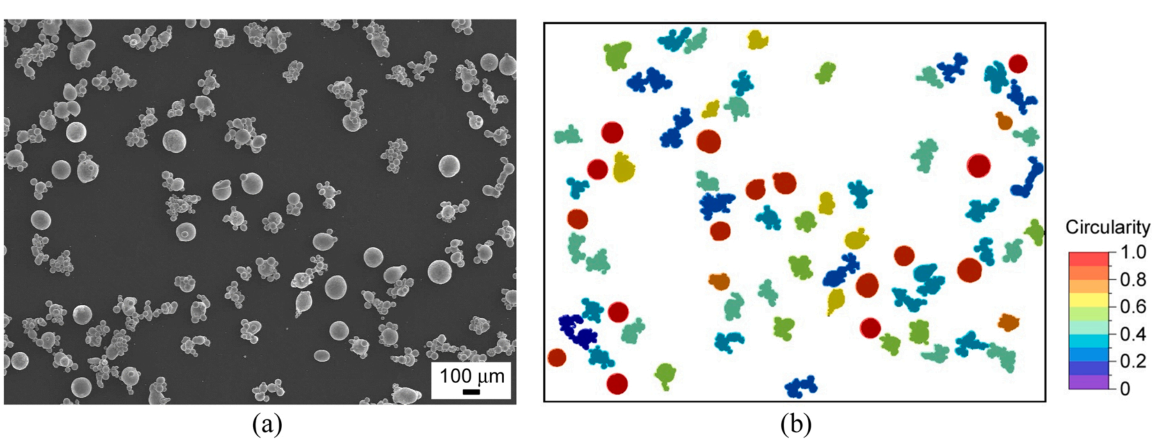

Fig. 2. Spatter particles: (a) SEM image and (b) colour plot of particle circularity.

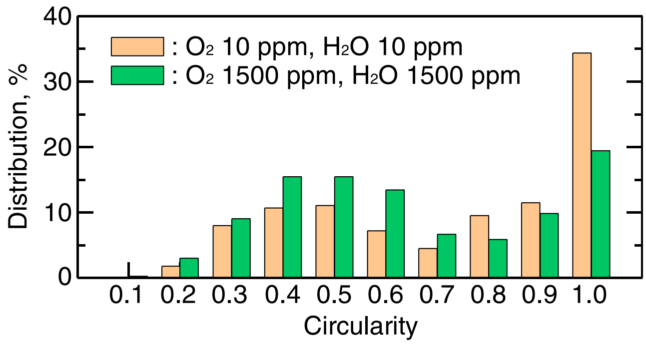

Fig. 3. Comparison of spatter particle circularity under different building environments.

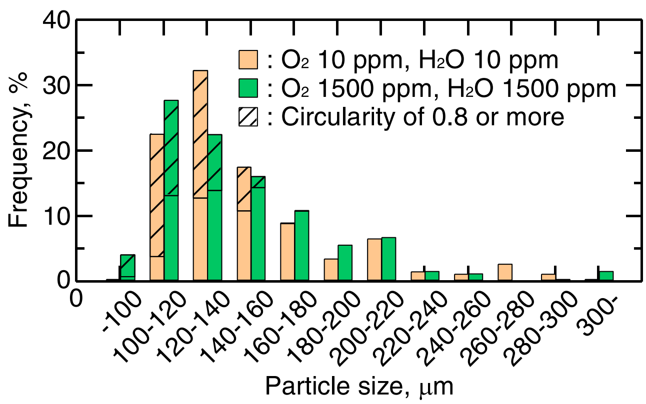

Fig. 4. Comparison of spatter particle size distribution under different building environments.

particles with a circularity of 0.8 or higher were 46% and 30%, respectively. In particular, for sizes of 100–140 μm, a large proportion of the particles featured a circularity of 0.8 or higher, under the oxygen concentration and humidity of 10 ppm.

Here, we discuss the effect of oxygen concentration and humidity in the building atmosphere on the circularity and size distribution of the spatter particles. Fig. 2 indicates that the spatter particles are composed of irregular particles and satellite-like particles, as compared with the virgin powder shown in Fig. 1. This can be attributed to the difference in the morphology of the ejected spatter particles and adsorption phenomena between the particle surfaces under a high oxygen concentration and humidity level. Hellwig et al. (2020) investigated that the influence of the oxygen concentration in the shielding gas on spatter behaviour and loss of mass during the laser processing using a precision balance and a high-speed camera and showed that the number of spatter particles increased with the oxygen concentration in the shielding gas, and the spherical spatter particles were formed under a low oxygen concentration due to a high surface tension. Meanwhile, Furumoto et al. (2022) evaluated the dynamic temperature behaviour around a melt pool during the building using a two-colour radiometric thermal imaging system and revealed that some spatter particles reached the powder bed in the liquid phase, which resulted in the formation of satellite-like spatter particles that then solidified owing to the adhesion of the loose metal powder. This suggests that the satellite-like particles are formed by adsorption between the spatter particle in the liquid phase and virgin powder due to either physisorption or chemisorption. In particular, the influence of the moisture in the building atmosphere on the physisorption associated with capillary and van der Waals forces between the particle surfaces can be significant. You and Wan (2013) proposed a mathematical model based on the fractal theory and Gaussian roughness distribution for capillary and van der Waals forces between the particle surfaces under various humidity and explained that the capillary force increases with that in the humidity, whereas the van der Waals force decreases. This means that the capillary force is more dominant at a high humidity. In addition, Pakarinen et al. (2005) suggested a method to numerically calculate the capillary bridge and the corresponding force and compared the measured value of the capillary force using an atomic force microscopy. They predicted the capillary force to be the highest when the particles are in contact with each other, and this force promotes the agglomeration of the particles when even a small amount of moisture is absorbed by the particles. This indicates that the capillary force has a greater effect on the spatter particles as they reach the powder bed rolls and solidify in contact with the virgin powder.

To summarize, it is assumed that the irregular spatter particles ejected and reached the powder bed under the high-oxygen concentration, and subsequently, satellite-like spatter particles were formed during solidification due to the adhesion of the virgin powder. Thereafter, the spatter particles absorbed the ambient moisture in the high-humidity atmosphere and agglomerated with the virgin powder owing to a high capillary force. As a result, a low oxygen concentration and humidity level enhanced high circularity and narrow particle size distributions of the spatter particles, as shown in Figs. 3 and 4. Thus, the variation in the circularity and particle size distributions of the spatter particles can be attributed to the interactions among the change in the morphology of spatter particles and adhesion force under a high oxygen concentration and humidity level.

Fig. 5 presents a comparison of the SEM and TEM images of the spatter particles and oxide film under different building environments. The state of the virgin metal powder prior to the building process is also depicted. The titanium alloy powder had a native oxide film of 4.0 nm on the powder surface; this was formed immediately after the plasma atomisation process. When the oxygen concentration and humidity were 10 ppm, the thickness of the oxide film on the spatter particles was 4.0 nm, identical to that in the case of the virgin metal powder. By

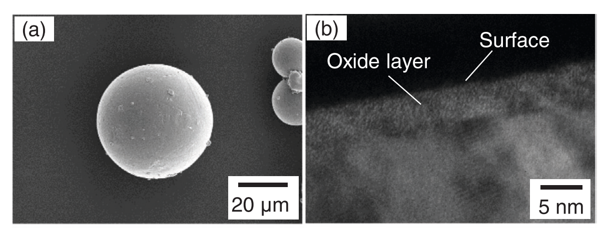

(a) Virgin metal powder and (b) its cross-section on the surface

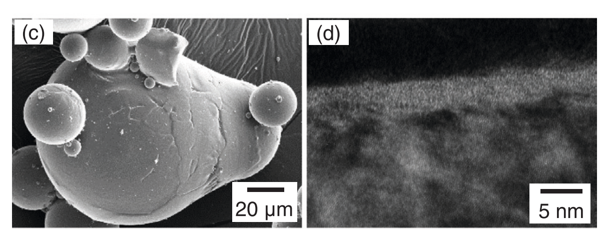

(c) Spatter particle and (d) its cross-section (O_2 and H_2O: 10 ppm)

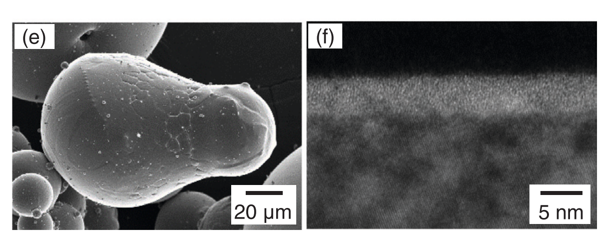

(e) Spatter particle and (f) its cross-section (O_2 and H_2O: 1,500 ppm)

Fig. 5. Comparison of spatter particle morphology and oxide film under different building environments.

contrast, the oxide film had a thickness of 4.7 nm when the oxygen concentration and humidity were 1500 ppm, i.e., it was 18% thicker than that under the condition of 10 ppm. The hot spatter particles were scattered in the form of a liquid phase from the laser-irradiated area and resulted in an increase in the oxide film thickness by dissolving oxygen.

Furthermore, Fig. 6 shows a comparison of the oxygen content in the spatter particles under different building environments. The oxygen content in the virgin powder (720 ppm) is also provided, for a comparison. The oxidation of the spatter particles accelerated with an increase in the oxygen and humidity levels inside the building chamber, particularly on increasing the humidity. In addition, the oxygen content in the spatter particles was similar to the sum of the results obtained on increasing the oxygen concentration and humidity levels. By contrast, when the oxygen and humidity levels were 10 ppm, the oxidation of the spatter particles was minimised, and the increase in the oxygen was suppressed to 15%, as compared with that in the virgin metal powder. This can be attributed to the PBF-LB/M processes implemented under high temperatures exceeding the melting point, and the oxygen and moisture in the building atmosphere can enhance the oxidation of the spatter particles during the solidification. Dong et al. (2017) determined the activation energies of oxidation to be 199 kJ/mol and 281 kJ/mol for temperatures above and below the beta transformation temperature (T_{β}), respectively, from an thermogravimetry and showed that the diffusion ability of oxygen in β-Ti with a body-centred cubic structure is greater than that in α-Ti with a hexagonal close-packed structure using an X-ray diffraction (XRD) and energy-dispersive X-ray spectroscope (EDS). In addition, Lu et al. (2022) identified the partial oxides of Si and Mn, which has a high affinity for oxygen and a low density of oxides, on the spatter surface through EDS analysis and revealed that oxides are formed during the flight and solidification of spatter particles. These results suggest a high oxygen concentration in the building atmosphere can accelerate oxidation reactions in the high-temperature spatter surface during the solidification. Meanwhile, the moisture in the building atmosphere can also affect the formation of the oxide film. Rouquerol et al. (2014) demonstrated that adsorption occurs whenever a solid surface is exposed to a liquid; simultaneously, either physisorption or chemisorption is induced owing to a reduction of the surface energy, and in particular, the moisture adsorbed on the surface results in the formation of a thicker external oxide film.

To summarize, high oxygen concentrations inside the building atmosphere enhanced the oxidation of the spatter particles during the flight and solidification, whereas high humidity supplied external oxygen as the moisture was absorbed by the spatter particles. Consequently, the increase in the thickness of the oxide film and oxygen content in the spatter particles was promoted by the interactions among these factors. Notably, controlling the humidity level inside the building atmosphere is more important than controlling the oxygen concentration, in terms of preventing the oxidation of spatter particles. Moreover, most spatter particles remained on the powder bed and blended into the virgin metal powder owing to the similar size distribution of the metal powders, although the oversized spatter particles could be removed during the sieving process employed for the reuse of the metal powder. Considering that it is difficult to physically remove the spatter particles from the powder bed, it is important to prepare a building environment wherein the characteristics of the spatter particles are identical to those of the metal powders to ensure the quality of built parts.

3.2. Influence of oxygen concentration and humidity in the building environment on built part properties

Fig. 7 shows a comparison of the oxygen content in the built part under different building environments. When the oxygen concentration and humidity were 10 ppm, the oxygen content in the built part was largely similar to that in the virgin powder. The oxygen content under a high oxygen concentration and humidity environment increased owing to the capture of oxygen from the atmosphere. In addition, the amount of oxygen supplied to the built parts was 950 ppm when the oxygen concentration and humidity in the building environment were 1500 ppm. This amount was 2.6 times lower than that of the spatter particles (2480 ppm), as shown in Fig. 6. By contrast, there were largely no differences between the oxygen concentration and the humidity in the building environment. This can be attributed to the difference in the liquid phase morphologies between the spatter particles and the built part. Furumoto et al. (2022) observed the formation of the satellite-like spatter particles using a high-speed camera and showed that spatter particles are generally ejected from the melt pool as liquid droplets and form satellite-like shapes owing to the adhesion of loose metal powder after reaching the powder bed, despite the cooling process during scattering. Meanwhile, the liquid phase during the part building is limited to the melt pool and its circumference. These results suggest that the capture of oxygen by the spatter particles or built parts occurs during the liquid phase, and the degrees of influence of the oxygen concentration and humidity in the building chamber on the capture of oxygen are similar.

Fig. 8 depicts a comparison of the hydrogen content in the built parts under different building environments. The hydrogen content increased under high-humidity levels. However, the increase in the hydrogen content was limited compared to the increase in the oxygen content, as shown in Fig. 7. This can be attributed to the difference in the solubility limit of oxygen and hydrogen, which are substitutional interstitial elements. Dietrich et al. (2020) determined that the oxygen content increased from 1308 ppm in virgin Ti–6Al–4V powder to 1848 ppm in the built part at an oxygen concentration of 977 ppm using an inert gas fusion method. Meanwhile, Bilgin et al. (2017) revealed that the hydrogen content of the as-built part was 0.0042 wt% and increased up to a maximum of 1.19 wt% with hydrogenation treatment at 923 K using XRD and XPS, which was caused by the structural transformation of the built part from a non-equilibrium needle-like α′ martensitic phase to β and δ (TiH_2) phases. These results indicate that oxygen is more easily picked up than hydrogen in the built part. In addition, Fig. 7 suggests that the presence of moisture in the building atmosphere can increase the oxygen concentration in the built part. Wouters et al. (1997)

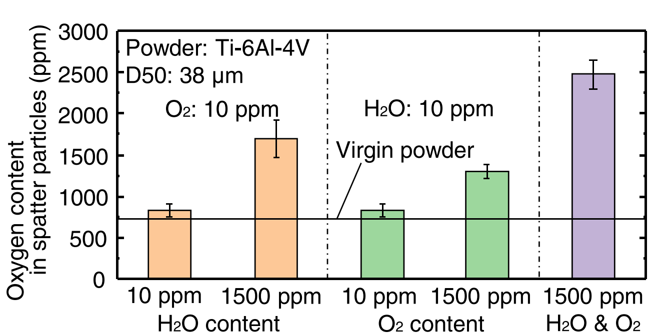

Fig. 6. Comparison of oxygen content in spatter particles under different building environments.

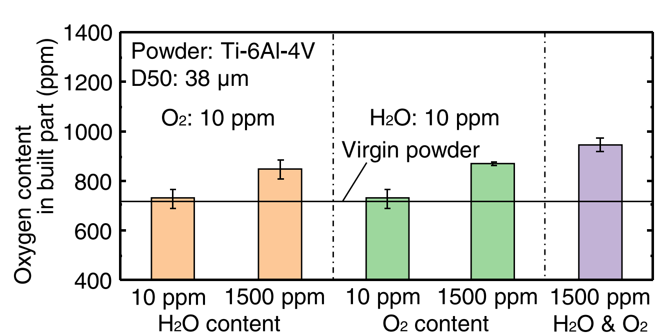

Fig. 7. Comparison of oxygen content in built part under different building environments.

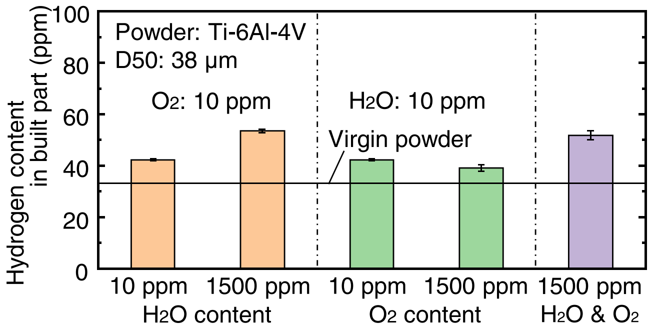

Fig. 8. Comparison of hydrogen content in built part under different building environments.

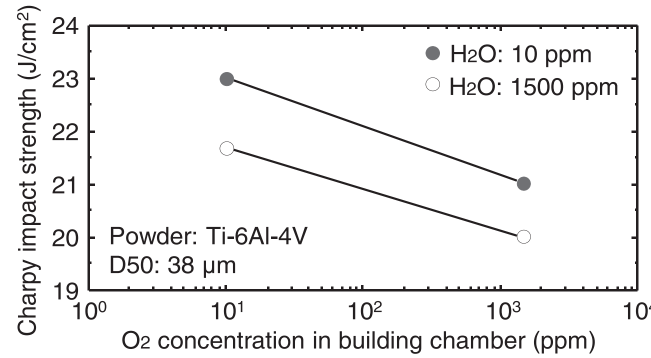

Fig. 10. Variation in Charpy impact strength with oxygen concentration.

showed that the oxidation of titanium was accelerated under high-temperature conditions in the presence of water vapour, primarily at a parabolic rate followed by linear growth, as long as water molecules were present using a thermogravimetry. They also revealed that oxidation in H_2O is accompanied by hydrogen transport through the formed TiO_2 layer using a glow discharge spectrometry, which was caused by a high diffusion coefficient of a substitutional hydroxide ion owing to its small radius ($OH^- = 95$ pm) compared to that of the oxide ion ($O_2^- = 140$ pm). Thus, the hydrogen content in the building atmosphere was saturated owing to the differences in the solubility limit, whereas the oxygen content increased with high oxygen concentration and humidity owing to differences in the ionic radius and diffusion rate. The amount of hydrogen pick-up could also increase in a high-humidity atmosphere owing to the heat accumulation during the building process with repeated laser irradiation.

Moreover, Fig. 9 presents a comparison of the tensile strength, 0.2% yield stress, and elongation of the built parts under different building environments. With an increase in the oxygen content in the built part, the tensile strength and 0.2% yield stress increased, whereas the elongation decreased. These results effectively represent the oxidation characteristics of titanium alloys. The mechanical properties of the built parts were related with the capture of oxygen by the built parts and remained unaffected by the oxygen and humidity in the chamber.

Fig. 10 demonstrates the variation in the Charpy impact strength with respect to the oxygen concentration and humidity in the building chamber. The impact strength of the built part was sensitive to both the oxygen and humidity in the building environment. When the oxygen and humidity was 10 ppm, the impact strength was 23.0 J/cm^2, whereas the strength decreased to 20.0 J/cm^2 under an oxygen concentration and humidity of 1500 ppm. In addition, the impact strength significantly decreased even when the oxygen and humidity were varied independently. The dissolution of hydrogen into the built part can cause hydrogen embrittlement via the formation of hydrides at the grain boundaries. Hardie and Ouyang (1999) showed that the crack propagation rate increases with the hydrogen content through the fatigue crack growth test in the range of the hydrogen content from 10 to 3000 ppm. They reported the transport of hydrogen by dislocations leads to accumulation at the α/β interface, resulting in hydride cracking. Meanwhile, Boyer and Spurr (1978) carried out a tensile test with a notch specimen treated under various heat conditions and revealed that the crack propagation rate increases with the oxygen content, which was attributed to the planar slip. These results indicate that the impact strength can help effectively understand the characteristics of built parts when the building environment varies slightly.

Fig. 11 shows a comparison of the optical microscope images of the polished built part surface under different building environments. The porosity of the built part was minimum when the oxygen concentration and humidity were 10 ppm; it increased from 0.02% to 0.07% when the oxygen and humidity level were increased to 1500 ppm. The oxidation of the built part was promoted by the capture of oxygen by the melt pool surface during the liquid phase and by the formation of an oxide film on the melt pool. Brillo et al. (2019) investigated the effect of the oxygen concentration on the melt flow dynamics by an electromagnetic levitation method and showed that the surface tension of the liquid melt pool decreased with an increase in the oxygen concentration and induced a change in the Marangoni convection, i.e., from an outward flow with a wide and shallow melt pool morphology to an inward flow with a narrow and deep melt pool morphology. Thus, high oxygen concentrations in the building environment can decrease the amount of overlap during layer building and result in the formation of irregular pores in built parts.

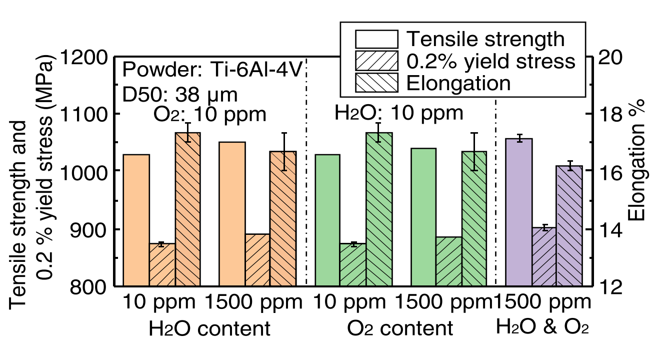

Fig. 9. Comparison of mechanical properties of built part under different building environments.

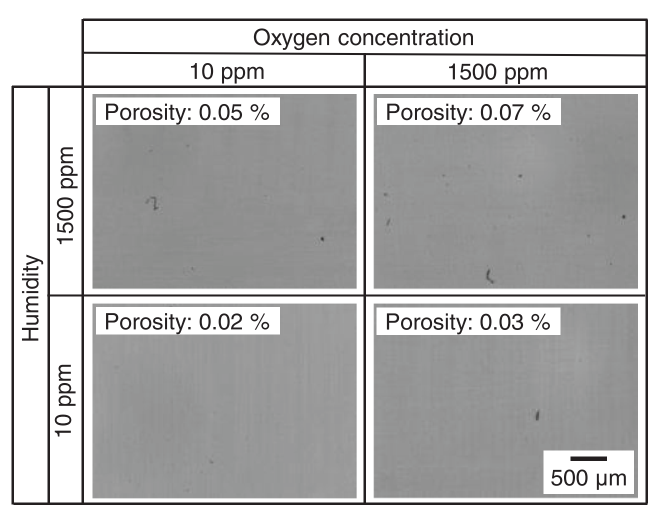

Fig. 11. Comparison of defect formation in built part under different building environments.

3.3. Influence of oxygen concentration and humidity in the building environment on reusability of metal powder

Fig. 12 presents a comparison of the oxygen content in the reused powder after reaching a building volume of 250,000 mm^3 under different building environments. The influence of humidity on the oxygen content in the reused powder was remarkable, despite the addition of the virgin powder at a ratio of 5:1 to the reused powder. The oxygen content under an oxygen concentration and humidity of 1500 ppm was 920 ppm, i.e., 25% higher than that under the condition of 10 ppm. In addition, the increase in the oxygen content of the reused powder was suppressed to 10 ppm, under the oxygen concentration and humidity of 10 ppm. These results suggest that an increase in the oxygen content can be attributed to the remaining spatter particles with a morphology similar to that of the reused powder, in addition to the increase in the thickness of the oxide film on the reused powder because of the increased temperature around the laser-irradiated area. The oxidation of the metal powder during the PBF-LB/M process is unavoidable. However, it can be minimised by minimising the oxygen concentration and humidity in the building chamber.

The oxygen concentration and humidity in the building atmosphere affected the metal powder behaviour at the melt pool, mechanical properties of the built part, and reusability of the metal powder. The adsorption of oxygen onto the metal powder could be attributed to the transition to the liquid phase during melt pool formation. The adsorption of oxygen onto the spatter particles was further promoted while moving in the liquid phase. By contrast, when the melt pool was formed, the active surface area, which is the principal factor for oxygen adsorption, was relatively small and resulted in the suppression of the oxidation of the melt pool, as compared with the spatter particles. In addition, it was difficult to remove the spatter particles via the sieving process because of the geometrical shapes. Thus, oxidation of the spatter particles should be suppressed to achieve the reusability of the metal powder. The removal of oxygen and humidity from the building environment is an important method to solve these issues; notably, controlling the humidity in the building chamber was found to be more important than controlling the oxygen concentration in terms of prevent the oxidation of the built parts and metal powder. Furthermore, the oxidation of the built parts and metal powder could be suppressed under an oxygen concentration and humidity of 10ppm.

4. Conclusions

In this study, Ti–6Al–4V powder was prepared in a PBF-LB/M system under different building environments, and the principal factors influencing the oxidation of the built part and metal powder were investigated. The following results were obtained:

1) Both the oxygen and humidity conditions inside the building chamber affected the building aspects and the reusability of the metal powder. Controlling the humidity in the building chamber was found to be more important than controlling the oxygen concentration to prevent the oxidation of the built part and metal powder.
2) Low oxygen concentrations and humidity levels resulted in high circularity and narrow size distributions of the spatter particles.
3) The Charpy impact strength was sensitive to the capture of oxygen and humidity by the built parts; thus, it can effectively help understand the building aspects under slightly different building environments.
4) High oxygen concentrations and humidity levels caused a change in the Marangoni convection, resulting in the formation of irregular pores. Hence, it is desirable to maintain the oxygen concentration and humidity below 10 ppm, to ensure the quality of the built parts.

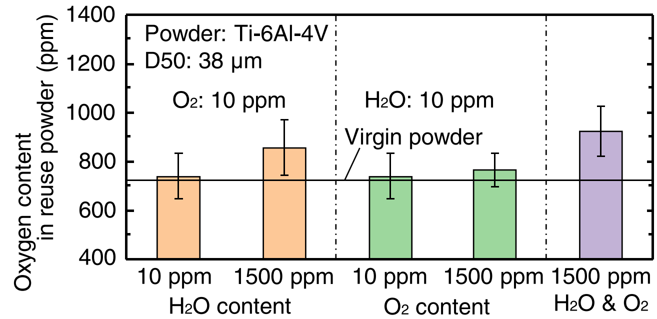

Fig. 12. Variation in oxygen content of reused powder under different building environments.

CRediT authorship contribution statement

Mitsugu Yamaguchi: Validation, Data curation, Writing – original draft, Visualisation. **Kotaro Kushima**: Investigation, Formal analysis. **Yushi Ono**: Investigation, Methodology. **Tomohiro Sugai**: Investigation, Methodology. **Tomohiro Oyama:** Conceptualisation, Resources. **Tatsuaki Furumoto**: Supervision, Project administration.

Declaration of Competing Interest

The authors declare that they have no known competing financial interests or personal relationships that could have appeared to influence the work reported in this paper.

Data availability

Data will be made available on request.

References

Bilgin, G.M., Esen, Z., Akın, Ş.K., Dericioglu, A.F., 2017. Optimization of the mechanical properties of Ti-6Al-4V alloy fabricated by selective laser melting using thermohydrogen processes. Mater. Sci. Eng. A 700, 574–582.
Boyer, R.R., Spurr, W.F., 1978. Effect of composition, microstructure, and texture on stress-corrosion cracking in Ti-61–4 V sheet. Metall. Trans. A 9, 1443–1448.
Brillo, J., Wessing, J., Kobatake, H., Fukuyama, H., 2019. Surface tension of liquid Ti with adsorbed oxygen and its prediction. J. Mol. Liq. 290, 111226.
Cordova, L., Bor, T., de Smit, M., Campos, M., Tinga, T., 2020. Measuring the spreadability of pre-treated and moisturized powders for laser powder bed fusion. Addit. Manuf. 32, 101082.
Dietrich, K., Diller, J., Dubiez-Le Goff, S., Bauer, D., Forêt, P., Witt, G., 2020. The influence of oxygen on the chemical composition and mechanical properties of Ti-6Al-4V during laser powder bed fusion (L-PBF). Addit. Manuf. 32, 100980.
Dong, E., Yu, W., Cai, Q., Cheng, L., Shi, J., 2017. High-temperature oxidation kinetics and behavior of Ti–6Al–4V alloy. Oxid. Met. 88, 719–732.
Furumoto, T., Oishi, K., Abe, S., Tsubouchi, K., Yamaguchi, M., Clare, A.T., 2022. Evaluating the thermal characteristics of laser powder bed fusion. J. Mater. Process. Technol. 299, 117384.
Hardie, D., Ouyang, S., 1999. Effect of hydrogen and strain rate upon the ductility of mill-annealed Ti6Al4V. Corros. Sci. 41 (1), 155–177.
Harkin, R., Wu, H., Nikam, S., Quinn, J., McFadden, S., 2020. Reuse of grade 23 Ti6Al4V powder during the laser-based powder bed fusion process. Metals 10 (12), 1700.
Hellwig, P., Schricker, K., Bergmann, J.P., 2020. Effect of reduced ambient pressure and atmospheric composition on material removal mechanisms of steel and aluminum by means of high-speed laser processing. Procedia CIRP 94, 487–492.
Hryha, E., Shvab, R., Bram, M., Bitzer, M., Nyborg, L., 2016. Surface chemical state of Ti powders and its alloys: Effect of storage conditions and alloy composition. Appl. Surf. Sci. 388, 294–303.
Li, X.P., O'Donnell, K.M., Sercombe, T.B., 2016. Selective laser melting of Al-12Si alloy: enhanced densification via powder drying. Addit. Manuf. 10, 10–14.
Lu, C., Zhang, R., Wei, X., Xiao, M., Yin, Y., Qu, Y., Li, H., Liu, P., Qiu, X., Guo, T., 2022. An investigation on the oxidation behavior of spatters generated during the laser powder bed fusion of 316L stainless steel. Appl. Surf. Sci. 586, 152796.
Pakarinen, O.H., Foster, A.S., Paajanen, M., Kalinainen, T., Katainen, J., Makkonen, I., Lahtinen, J., Nieminen, R.M., 2005. Towards an accurate description of the capillary force in nanoparticle-surface interactions. Model. Simul. Mater. Sci. Eng. 13, 1175–1186.
Pauzon, C., Dietrich, K., Forêt, P., Dubiez-Le Goff, G., Hryha, E., Witt, G., 2021. Control of residual oxygen of the process atmosphere during laser-powder bed fusion processing of Ti-6Al-4V. Addit. Manuf. 38, 101765.

Quintana, O.A., Alvarez, J., Mcmiullan, R., Tong, W., Tomonto, C., 2018. Effects of reusing Ti–6Al–4V powder in a selective laser melting additive system operated in an industrial setting. J. Miner. Met. Mater. Soc. 70, 1863–1869.

Rouquerol, F., Rouquerol, J., Sing, K.S.W., Maurin, G., Llewellyn, P., 2014. Adsorption by Powders and Porous Solids, second edition.,. Academic Press,, Oxford, pp. 1–24.

Schmidt, M., Merklein, M., Bourell, D., Dimitrov, D., Hausotte, T., Wegener, K., Overmeyer, L., Vollertsen, F., Levy, G.N., 2017. Laser based additive manufacturing in industry and academia. CIRP Ann. Manuf. Technol. 66 (2), 561–583.

Seyda, V., Kaufmann, N., Emmelmann, C., 2012. Investigation of aging processes of Ti-6Al-4 V powder material in laser melting. Phys. Proc. 39, 425–431.

Shipley, H., McDonnell, D., Culleton, M., Coull, R., Lupoi, R., O'Donnell, G., Trimble, D., 2018. Optimisation of process parameters to address fundamental challenges during selective laser melting of Ti–6Al–4V: A Review. Int. J. Mach. Tools Manuf. 128, 1–20.

Weingarten, C., Buchbinder, D., Pirch, N., Meiners, W., Wissenbach, K., Poprawe, R., 2015. Formation and reduction of hydrogen porosity during laser melting of AlSi10Mg. J. Mater. Process. Technol. 221, 112–120.

Williams, R., Bilton, M., Harrison, N., Fox, P., 2021. The impact of oxidised powder particles on the microstructure and mechanical properties of Ti–6Al–4V processed by laser powder bed fusion. Addit. Manuf. 46, 102181.

Wouters, Y., Galerie, A., Petit, J.-P., 1997. Thermal oxidation of titanium by water vapour. Solid State Ion. 104, 89–96.

Yan, M., Dargusch, M.S., Ebel, T., Qian, M., 2014. A transmission electron microscopy and three-dimensional atom probe study of the oxygen-induced fine microstructural features in as-sintered Ti–6Al–4V and their impacts on ductility. Acta Mater. 68, 196–206.

You, S., Wan, M.P., 2013. Mathematical models for the van der Waals force and capillary force between a rough particle and surface. Langmuir 29, 9104–9117.